© 2020. Published by The Company of Biologists Ltd | Journal of Cell Science (2020) 133, jcs236935. doi:10.1242/jcs.236935

RESEARCH ARTICLE

Recycling endosomes attach to the trans-side of Golgi stacks in *Drosophila* and mammalian cells

Syara Fujii[1], Kazuo Kurokawa[2], Ryota Inaba[1], Naoki Hiramatsu[1], Tatsuya Tago[1], Yuri Nakamura[1], Akihiko Nakano[2], Takunori Satoh[1,*] and Akiko K. Satoh[1,*]

ABSTRACT

Historically, the trans-Golgi network (TGN) has been recognized as a sorting center of newly synthesized proteins, whereas the recycling endosome (RE) is a compartment where endocytosed materials transit before being recycled to the plasma membrane. However, recent findings revealed that both the TGN and RE connect endocytosis and exocytosis and, thus, are functionally overlapping. Here we report, in both *Drosophila* and microtubule-disrupted HeLa cells, that REs are interconvertible between two distinct states, namely Golgi-associated REs and free REs. Detachment and reattachment of REs and Golgi stacks are often observed, and newly synthesized glycosylphosphatidylinositol-anchored cargo protein but not vesicular stomatitis virus G protein is transported through these two types of RE. In plants, there are two types of TGN – Golgi-associated TGN and Golgi-independent TGN. We show that dynamics of REs in both *Drosophila* and mammalian cells are very similar compared with those of plant TGNs. And, together with the similarity on the molecular level, our results indicate that fly and mammalian REs are organelles that are equivalent to TGNs in plants. This suggests that the identities and functional relationships between REs and TGNs should be reconsidered.

KEY WORDS: Recycling endosomes, Trans-Golgi network, TGN

INTRODUCTION

The Golgi apparatus has a pivotal role in the secretory pathway, as it is responsible for modification and sorting of secretory proteins and lipids to multiple destinations within the cell (Klumperman, 2011; Papanikou and Glick, 2014). The basic structural unit of the Golgi apparatus are the Golgi stacks, comprising several flattened membrane-enclosed compartments, i.e. cisternae and tubules. Golgi stacks are scattered in the cytoplasm of plant, *Caenorhabditis elegans* and *Drosophila* cells. In mammalian cells, however, several or more Golgi stacks are connected through lateral tubules to form Golgi ribbons, which localize to the periphery of the microtubule organizing center (MTOC) (Gosavi and Gleeson, 2017; Wei and Seemann, 2017). Golgi stacks are polarized, that is newly synthesized secretory proteins from the endoplasmic reticulum (ER) enter cis and exit trans. The trans-Golgi network (TGN) is located at the trans-most side of the Golgi stacks and is considered as a hub, where exocytic and endocytic pathways meet and act as a sorting center (Hierro et al., 2015; Makaraci and Kim, 2018). Although only reported in plants, the TGN can be divided into two types, Golgi-associated TGN (GA-TGN) and Golgi-independent TGN (GI-TGN, hereafter referred to as free-TGN) (Kang et al., 2011; Uemura et al., 2014; Viotti et al., 2010). Free-TGN compartments are defined as cisternae that have peeled-off from the Golgi stacks, as observed by using electron microscopy (Kang et al., 2011) or as the membrane that has detached from Golgi stacks by using live cell imaging (Kang et al., 2011; Uemura and Nakano, 2013; Uemura et al., 2014; Viotti et al., 2010).

The recycling endosome (RE) has first been defined as the perinuclear compartment involved in the slow recycling of transferrin endocytosed from the plasma membrane (Mayor et al., 1993; Yamashiro and Maxfield, 1987). Later, it was reported that the RE also receives newly synthesized exocytic cargos from the Golgi apparatus and, therefore, the RE is now recognized as a hub of endocytic and exocytic pathways (Ang et al., 2004; Lock and Stow, 2005). REs are often closely associated with the MTOC in mammalian cells (Sakai et al., 1991; Ullrich et al., 1996), most prominently in COS1 cells, in which Golgi ribbons surrounding the circular RE and MTOC appear like a fried egg (Misaki et al., 2010).

In this study, we report that REs present in two distinct states – i.e. as Golgi-associated REs (GA-REs) and Golgi-independent REs (free-REs) – in *Drosophila* cells and in HeLa cells with disrupted microtubules. Moreover, cargo seems to pass through these two REs before reaching the plasma membrane. GA-REs and free-REs are interconvertible, and dynamics of REs reveal strong similarity to those of TGNs in plants. Collectively, these results indicate that the two states of RE exist in both mammals and flies, and that plant TGNs and animal REs are homologous organelles.

RESULTS

RE markers are associated with the trans-side of Golgi stacks in *Drosophila* tissue

In photoreceptors of flies at late pupal stage, the most widely accepted RE marker, i.e. Rab11 (Goldenring, 2015; Ullrich et al., 1996; van Ijzendoorn, 2006), is associated with Golgi stacks (Fig. 1A, Fig. S1A arrowheads) and post-Golgi vesicles at the rhabdomere base (Fig. 1A, Fig. S1A arrows) (see Iwanami et al., 2016; Otsuka et al., 2019; Satoh et al., 2005). For a more-detailed analysis of Rab11 associated with Golgi stacks, we examined retinas at early pupal stage, which comprise larger Golgi stacks compared to those at late pupal stage. As reported previously (Riedel et al., 2016; Yamamoto-Hino et al., 2012), Golgi markers of cis- (GM130), medial- (p120) and trans-cisternae (GalT::ECFP), as well as TGN (Golgin245) markers, are localized in a reasonable arrangement (Fig. 1E,G). In this context, Rab6 localization was found as spanning broadly from the trans-Golgi to the TGN (Fig. 1G), as reported previously (Iwanami et al., 2016; Satoh et al.,

[1]Program of Life and Environmental Science, Graduate School of Integral Science for Life, Hiroshima University, 1-7-1 Kagamiyama, Higashi-Hiroshima, Hiroshima 739-8521, Japan. [2]Live Cell Super-Resolution Imaging Research Team, RIKEN Center for Advanced Photonics, 2-1 Hirosawa, Wako, Saitama 351-0198, Japan.

*Authors for correspondence (aksatoh@hiroshima-u.ac.jp; tsatoh3@hiroshima-u.ac.jp)

K.K., 0000-0003-3549-4795; A.N., 0000-0003-3635-548X; T.S., 0000-0003-0340-5532; A.K.S., 0000-0001-7336-6642

Received 23 July 2019; Accepted 13 January 2020

Journal of Cell Science (2020) 133, jcs236935. doi:10.1242/jcs.236935

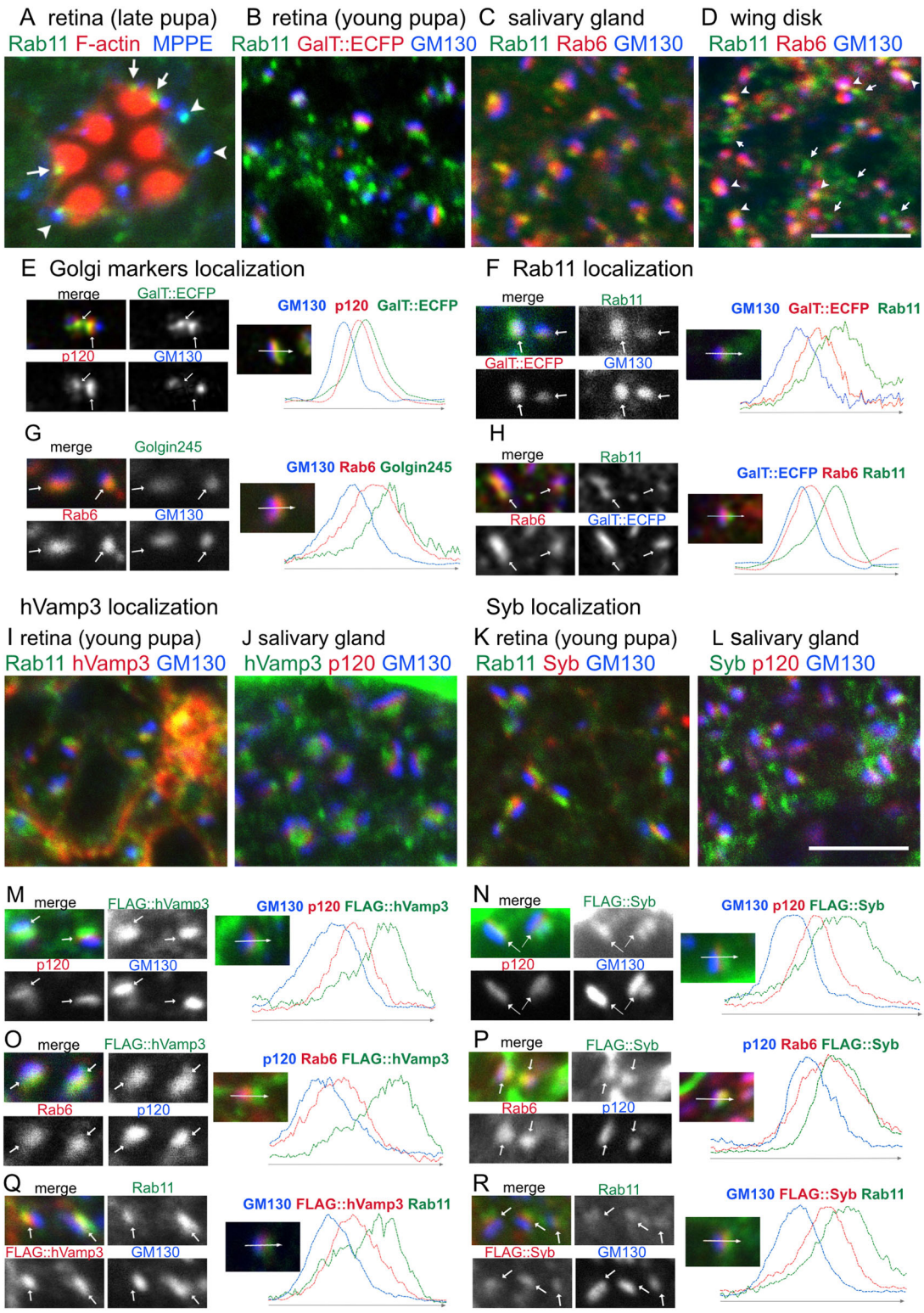

Fig. 1. REs attach to the trans-side of Golgi stacks in fly tissues. (A) Retina from late pupa immunostained with anti-Rab11 (green) and anti-MPPE (blue) antibodies, and phalloidin (red). Arrowheads indicate the Golgi stacks associated with Rab11. Arrows indicate Rab11-positive post-Golgi vesicles. (B) Retina from early pupa expressing GalT::ECFP (red), immunostained with anti-Rab11 (green) and anti-GM130 (blue) antibodies. (C,D) Immunostaining of salivary gland (C) and wing disk (D) using anti-Rab11 (green), anti-Rab6 (red) and anti-GM130 (blue) antibodies. Arrowheads indicate Rab11 association with the Golgi stacks. Arrows indicate free Rab11-positive foci. (E-H,M-R) Left panels are examples of triple-stained Golgi stacks or REs using the indicated antibodies or fluorescent proteins. Arrows indicate medial Golgi. Plots show signal intensities from image on the left. Signal intensity was measured along the arrow (representing 1.5 µm) in inset, graph shows the overlap between channels. (I) Retina from early pupa expressing FLAG::hVamp3 (red) immunostained for Rab11 (green) and GM130 (blue). (J) Salivary gland expressing FLAG::hVamp3 (green) immunostained for p120 (red) and GM130 (blue). (K) Retina from early pupa expressing FLAG::Syb (red) immunostained for Rab11 (green) and GM130 (blue). (L) Salivary gland expressing FLAG::Syb (green) immunostained for p120 (red) and GM130 (blue). Scale bars: 5 µm.

Journal of Cell Science (2020) 133, jcs236935. doi:10.1242/jcs.236935

2005). Rab11 also accumulated at the trans-side of the Golgi stack (Fig. 1B,F, Fig. S1B) but further from the Golgi stacks compared with Rab6 (Fig. 1H). Cells in the salivary gland comprised well-developed Golgi stacks associated with Rab11 on their trans-side (Fig. 1C, Fig. S1C); by contrast, cells in the wing imaginal disks had small Golgi stacks mostly accompanied by Rab11 on their trans-side (Fig. 1D, Fig. S1D arrowheads) and also many Rab11-positive puncta without any Golgi association (Fig. 1D, Fig. S1D arrows). Thus, association of Rab11 with the trans-side of Golgi stacks is common in *Drosophila* cells.

As Rab11 localizes to the trans-side of Golgi stacks, we investigated the localization of other RE markers, human Vamp3 (hVamp3) and its *Drosophila* ortholog synaptobrevin (Syb) (Misaki et al., 2010; Rosenbaum et al., 2014). In retinas at early pupal stage and in salivary glands of third instar larvae, that express FLAG::hVamp3 or FLAG::Syb, both tagged proteins mainly localized to the plasma membrane but also concentrated in the cytoplasmic foci predominantly associated with the trans-side of the Golgi stacks (Fig. 1I–R, Fig. S1E-H). Both FLAG::hVamp3 and FLAG::Syb were slightly displaced towards the cis-side compared to Rab11 (Fig. 1Q,R). These results indicate that Golgi stacks are accompanied by REs on the trans-side, although there are also free-REs in *Drosophila*.

RE markers partially colocalize with TGN markers in *Drosophila* tissues

Since the TGN is located at the trans-side of the Golgi stack, we next investigated the relationship between TGN and RE markers. The well-established TGN markers, Golgin245 and AP1γ (Burgess et al., 2011; Hirst et al., 2009; Riedel et al., 2016), localized to the same side of the GalT::ECFP signal, which is presumed to be on the trans-side. Golgin245 was closely associated with GalT::ECFP but AP1γ was further away from GalT::ECFP (Fig. 2A,E, Fig. S1I). We compared localization of Rab11 with that of the two TGN markers in retinas at early pupal stage and in salivary glands. Rab11 localized to the trans-side of both Golgin245 and AP1γ. Rab11 was completely separated from Golgin245 but mainly colocalized with AP1γ (Fig. 2B,C,F,G, Fig. S1J,K). Next, we compared the localization of FLAG::hVamp3 with the TGN markers. FLAG::hVamp3 localized to the trans-side of Golgin245 but to the cis-side of AP1γ (Fig. 2D,H-J, Fig. S1L). These results indicated that *Drosophila* RE is an organelle equivalent to the TGN or one that is slightly more matured than TGN.

REs localized to the trans-side of Golgi stacks in *Drosophila* S2 cells

By using electron microscopy, we also investigated the localization of RE markers in Schneider 2 (S2) cells derived from *Drosophila* embryos (Schneider, 1972). We have recently reported that Parcas (Pcs) is the predominant Rab11-GEF in fly photoreceptors and intensively colocalizes with Rab11 (Otsuka et al., 2019). In S2 cells, V5::Pcs localized to the trans-side of Golgi stacks (Fig. 3A), together with HA::Rab11 (Fig. 3B–D). By using the genetic EM-tag ascorbate peroxidase 2 (APEX2; Martell et al., 2017), we also found Pcs localization to the cytoplasmic surface of 150–300 nm distorted vesicles or cisternae, which often associate with Golgi stacks (Otsuka et al., 2019). To clarify Pcs localization in regard to cis–trans polarity of Golgi stacks, we performed double-APEX-labeling of GalT and Pcs. As the radicals generated by APEX2 did not spread across the membrane, DAB-deposition generated by GalT::APEX2::EGFP is expected to be limited to the lumen of trans-Golgi cisternae (Fig. 3E) and, thus, distinguishable from the DAB-depositions generated by myc::APEX2::Pcs, which localized to the cytoplasmic face (Fig. 3F). As expected, the electron-dense DAB-depositions were found both inside the cisternae and on the surface of the 150–300 nm distorted vesicles (Fig. 3G–I). These two types of DAB-deposition often localized closely (Fig. 3H,I). Superficial DAB staining was also observed on the free vesicles with a diameter of ∼200 nm (Fig. 3G (as elsewhere) arrows), although associated Golgi stacks could just be missing in the electron micrograph of the thin section. These EM observations were in accordance with observations using confocal microscopy (Figs 1, 2 and 3A–D) and suggest that the *Drosophila* cells have two types of RE, i.e. GA-REs and free-REs.

Live imaging of RE and Golgi stacks in S2 cells

Next, the dynamic relationship between GA-REs and free-REs visualized by trans-Golgi (GalT::EGFP) and RE markers (tdTomato::Rab11) in S2 cells was examined using super resolution confocal live imaging microscopy (SCLIM) (Kurokawa et al., 2013, 2019) (Fig. 3J–L). Although there were some free-REs (Fig. 3J,L arrows), most of the Golgi stacks were continuously accompanied by REs (Fig. 3J arrowheads, Movie 1). REs occasionally detached from Golgi (Fig. 3K,L) or attached to Golgi stacks (Fig. 3K). REs themselves also detached from or attached to each other (Fig. 3L arrows, Movie 1).

REs localize to the trans-side of Golgi stacks in mammalian cells

In mammalian cells, the Golgi stacks and REs are gathered close to the MTOC through dynein-based motility on microtubules (Fig. 4A) (Corthésy-Theulaz et al., 1992; Goldenring, 2015; Granger et al., 2014; Horgan et al., 2010; Sakai et al., 1991; Ullrich et al., 1996; van Ijzendoorn, 2006; Wei and Seemann, 2017). The MT polymerization inhibitor nocodazole is well known to disperse in both Golgi stacks and REs through the cytoplasm (Fig. 4B); however, the spatial relationship of these two organelles has not been precisely investigated. Interestingly, EGFP::hVamp3 was clearly associated with the trans-side of Rab6-positive Golgi stacks (Fig. 4B,C). Endogenous hVamp3, transferrin receptor (TfR) and tdTomato::Rab11a were also attached to the trans-side of Golgi stacks (Fig. 4D–F,H–J, Fig. S2A–C). To test whether the Golgi-associated structures positive for RE markers are, indeed, functional REs, we investigated the transport of endocytosed transferrin (Tf) to these structures. In MT-disrupted HeLa cells, after 20 min of uptake and 10 min of chase, Alexa Fluor-568-conjugated Tf (Tf-568) localized to the trans-side of Golgi stacks (Fig. 4G,K, Fig. S2D). These results strongly indicate that Golgi stacks in MT-disrupted HeLa cells are associated with functional REs. Therefore, we refer to this structure in MT-disrupted HeLa cells as Golgi-associated recycling endosome (GA-RE).

Furthermore, we quantified the spatial association of REs and Golgi stacks in nocodazole-treated HeLa cells, in which 73% (76/106, ±9.2%) of GalT::mTq2-defined trans-Golgi-cisternae were closely associated with TfR-defined REs (Fig. 4L). By contrast, 47.4% (76/162, ±2.9%) of TfR-defined REs closely associated with GalT::mTq2-defined trans-Golgi-cisternae (Fig. 4M), whereas 52.6% (86/162, ±2.9%) were free from Golgi markers (Fig. 4M) at a probability higher than free Golgi stacks (27.1%, 30/106, ±9.2%, Fig. 4L). Similarly, GalT::mTq2-defined trans-Golgi-cisternae often associated with Vamp3-defined REs (77.5%, 139/179, ±2.7%, Fig. 4O). These results indicated that >70% of Golgi stacks are accompanied by REs; however, a substantial amount of free-REs exist (Fig. 4L–P).

Journal of Cell Science (2020) 133, jcs236935. doi:10.1242/jcs.236935

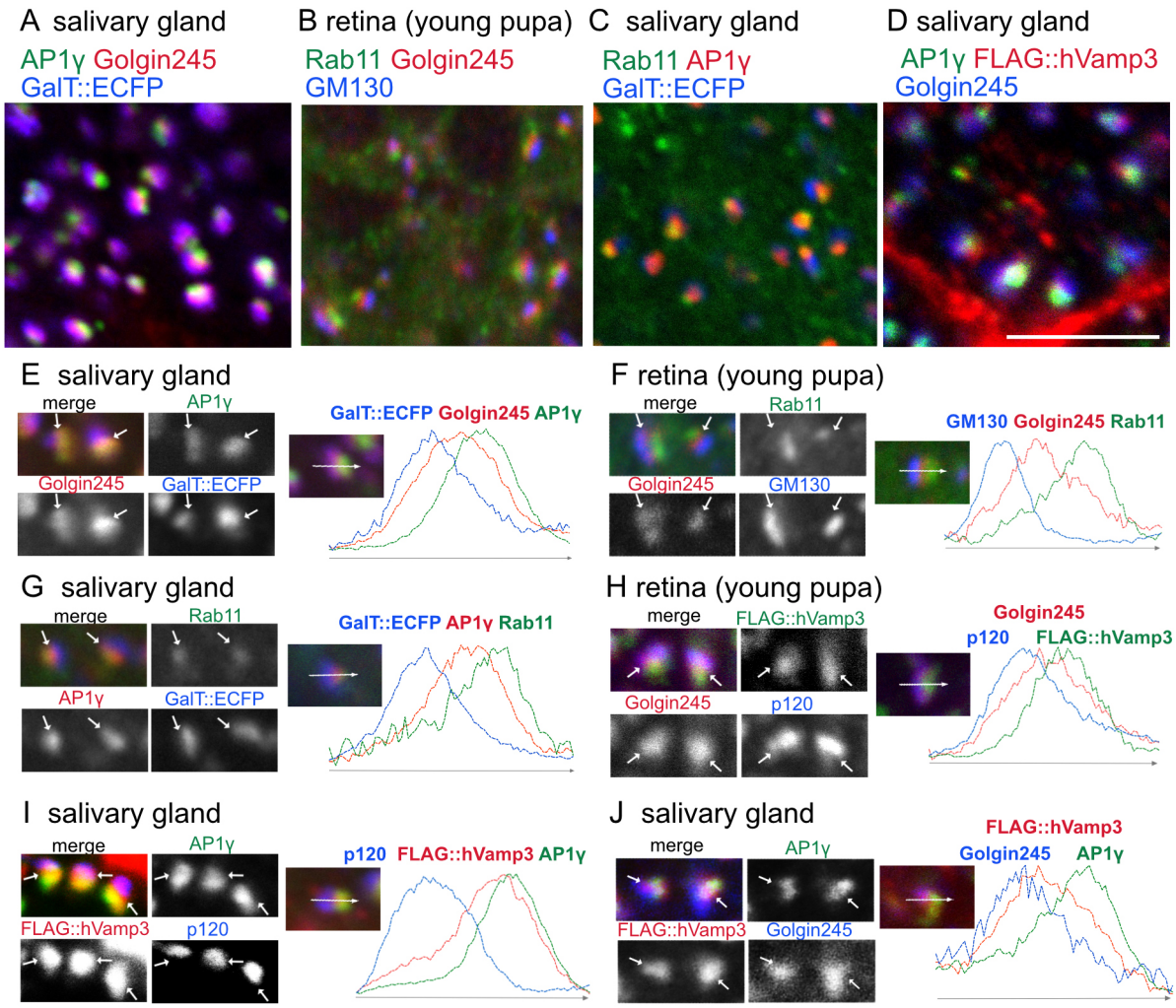

Fig. 2. Location of REs and TGN markers in fly tissues. (A) Immunostaining of salivary gland expressing GalT::ECFP (blue) for AP1γ (green) and Golgin245 (red). (B) Retina from early pupa immunostained with anti-Rab11 (green), anti-Golgin245 (red) and anti-GM130 (blue) antibodies. (C) Salivary gland expressing GalT::ECFP (blue) immunostained for Rab11 (green) and AP1γ (red). (D) Salivary gland expressing FLAG::Vamp3 (red) immunostained for AP1γ (green) and Golgin245 (blue). (E–J) Left panels are examples of triple-stained Golgi stacks or REs (arrows) using the indicated antibodies or fluorescent proteins. Plots show signal intensities from image on the left. Signal intensity was measured along the arrow (representing 1.5 µm) in inset, graph shows the overlap between channels. Scale bars: 5 µm (A–D).

RE markers partially colocalize with TGN markers in HeLa cells

We next investigated the relationship between TGN and RE markers in HeLa cells. EGFP::hVamp3 located further to the trans-side of Golgi stacks compared with the well-established TGN marker Golgin245 (Fig. 5A,E, Fig. S2E) (Gleeson et al., 1996). This TGN marker similarly localized between another RE maker TfR::tdTomato and a trans-Golgi marker, GalT::iRFP (Fig. 5B,F, Fig. S2F). In good agreement with this observation, both mRuby3::Rab11 and TfR::tdTomato localized to the trans-side of another TGN marker Vti1a (Fig. 5C,D,G–I, Fig. S2G,H) (Kreykenbohm et al., 2002). Interestingly, Vti1a also colocalized with mRuby3::Rab11 and TfR::tdTomato on the membrane without GalT::iRFP (Fig. 5I arrowheads). Another TGN marker, γ adaptin (Chakrabarti et al., 1993; Guo et al., 2013), also colocalized with TfR::tdTomato on both GalT::iRFP-positive and -negative structures (Fig. 5J). These results support the finding that mammalian REs, like *Drosophila* REs, are organelles that are equivalent to the TGN or to a slightly matured form of the TGN.

Live imaging of RE and Golgi stacks in HeLa cells

The dynamics of REs and Golgi stacks in MT-disrupted HeLa cells were observed by using SCLIM. Many GalT::EGFP-defined trans-Golgi-cisternae accompanied by REs were visualized by either tdTomato::Rab11a (Fig. 6A arrows, D–G arrowheads) or TfR::tdTomato (Fig. 6H). Most of these GA-REs were found to be in close proximity to trans-Golgi cisternae during the observation time (2.5 min; Movie 2). In MT-disrupted HeLa cells, Golgi stacks rarely moved (Fig. 6A,B, Movie 2). By contrast, either TfR-defined or Rab11a-defined free-REs were moving around the cytoplasm, often fusing to and separating from each other (Fig. 6A,C, Movies 2 and 4).

Interestingly, some of the GA-REs moved away from the trans-Golgi-cisternae (Fig. 6D arrow, E,H, Movie 3). In some cases, detached REs showed dynamic behaviors, such as re-association with original and other trans-Golgi-cisternae or fusion with free-REs (Fig. 6F, Movies 3 and 4). Furthermore, from some Rab11a-defined GA-REs, small foci of tdTomato-Rab11a appeared and quickly moved away, presumably representing the vesicles budding out of GA-REs (Fig. 6G, Movie 3).

Journal of Cell Science (2020) 133, jcs236935. doi:10.1242/jcs.236935

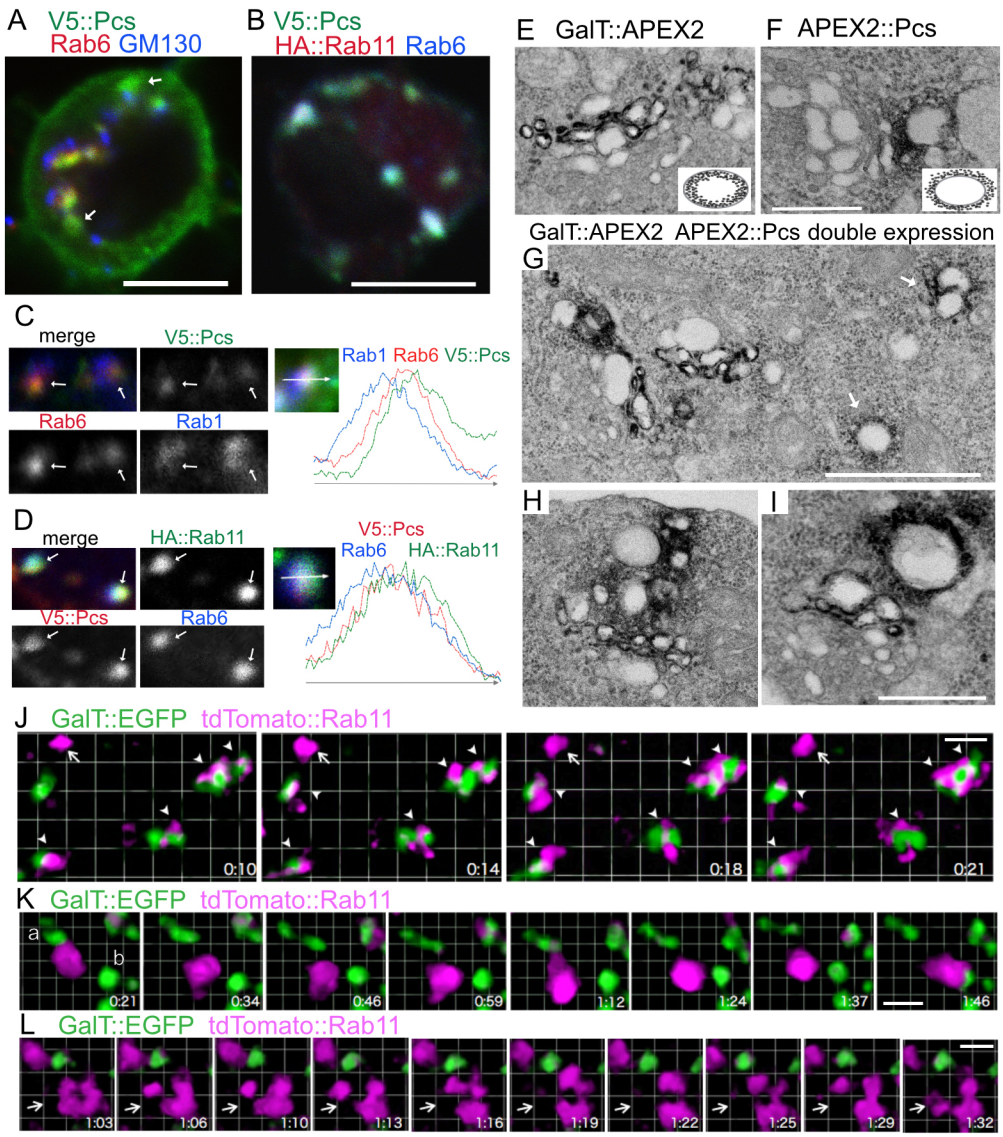

Fig. 3. REs attach to the trans-side of Golgi stacks in S2 cells. (A) S2 cells expressing V5::Pcs (green) immunostained by anti-Rab6 (red) and anti-GM130 (blue) antibodies. Arrows indicate free-RE. (B) S2 cells expressing V5::Pcs and HA::Rab11 immunostained with anti-V5 (green), anti-HA (red) and anti-Rab6 (blue) antibodies. (C,D) Left panels are examples of triple-stained Golgi stacks or REs (arrows) by indicated antibodies or fluorescent proteins. Plots show signal intensities from image on the left. Signal intensity was measured along the arrow (representing 1.5 µm) in inset, graph shows the overlap between channels. (E–I) Electron micrographs of S2 cells expressing GalT::APEX2::EGFP (E), myc::APEX2::Pcs (F) or both (G–I). APEX2 localization was visualized by osmium-enhanced DAB-depositions. Insets in E and F indicate schematic for osmium-enhanced DAB-depositions formed by GalT::APEX2::EGFP and myc::APEX2::Pcs, respectively. Arrows in G present possible free-REs with DAB-depositions of myc::APEX2::Pcs. (J–L) Live imaging of S2 cells expressing GalT::EGFP (green) and tdTomato::Rab11 (magenta). Arrowheads indicate GA-RE, arrows indicate free-RE. Time is provided as min:s. Scale bars: 5 µm (A,B), 1.5 µm (E,F), 500 nm (G), 1 µm (H–L).

Glycosylphosphatidylinositol-anchored protein but not vesicular stomatitis virus G accumulates at Golgi-attached RE

To investigate the functional significance of RE-association with Golgi stacks, we closely examined whether cargo proteins localize to GA-REs. We used a RUSH system for synchronous release of cargos from the ER by biotin-addition. We first confirmed that the time courses of the cargo transports we observed were relevant to those of previous reports; both ss::SBP::EGFP::glycosylphosphatidylinositol (GPI) and vesicular stomatitis virus G (VSV-G) tagged to VSV-G::SBP::EGFP (VSV-G) reached the Golgi stacks at around 10 min, and most of the cargo localized to the plasma membrane by ∼1 h after biotin addition, although there was still some cargo staining on the Golgi stacks (Fig. 7A,B). We closely compared cargo localizations for GPI at 25 min with VSV-G 28 min after addition of biotin, with those of the trans-Golgi marker (GalT::iRFP) and RE-marker (mRuby3::Rab11) using SCLIM (Fig. 7C,D). GPI strongly accumulated at GA-RE, and some GPI also was located at free-REs (Fig. 7C, Movie 5). By contrast, VSV-G localization to the REs was limited, although it was observed near GalT::iRFP and mRuby3::Rab11 (Fig. 7D, Movie 5). Quantification of the ratio of RE-localization area over total staining area for both GPI and VSV-G confirmed that VSV-G localization to GA-RE was significantly higher than VSV-G localization to GA-RE (Fig. 7E).

Dynamic behaviors of REs were still visible in HeLa cells expressing either GPI or VSV-G (Fig. 7F–I), whereby GA-RE and free-RE were constantly attached to and detached from each other. In addition, GPI on GA-REs also intensively interacted with GPI on free-REs (Fig. 7F,G). A GPI-loaded tubule was visible between the GA-RE and free RE [Fig. 7G, movie frames at (min:s): 1:40, 4:30 and 5:30]. Interestingly, the amount of GPI on GA-REs gradually reduced during the interaction between GPI on a GA-RE and GPI on a free-RE in Fig. 7G, suggesting that GPI moved from GA-RE to free-RE. We did not observe these interactions for VSV-G (Fig. 7H,I). These results strongly indicate that GPI but not VSV-G is transported by GA-REs.

DISCUSSION

REs attached to the trans-side of Golgi stacks in both fly and mammalian cells

By using confocal microscopy, SCLIM and EM, we showed that most Golgi stacks are accompanied by so-called RE markers on their trans-side, although RE markers also localize to separate positions from Golgi stacks in both fly and nocodazole-treated mammalian cells. It has previously been reported that the Rab11–

Journal of Cell Science (2020) 133, jcs236935. doi:10.1242/jcs.236935

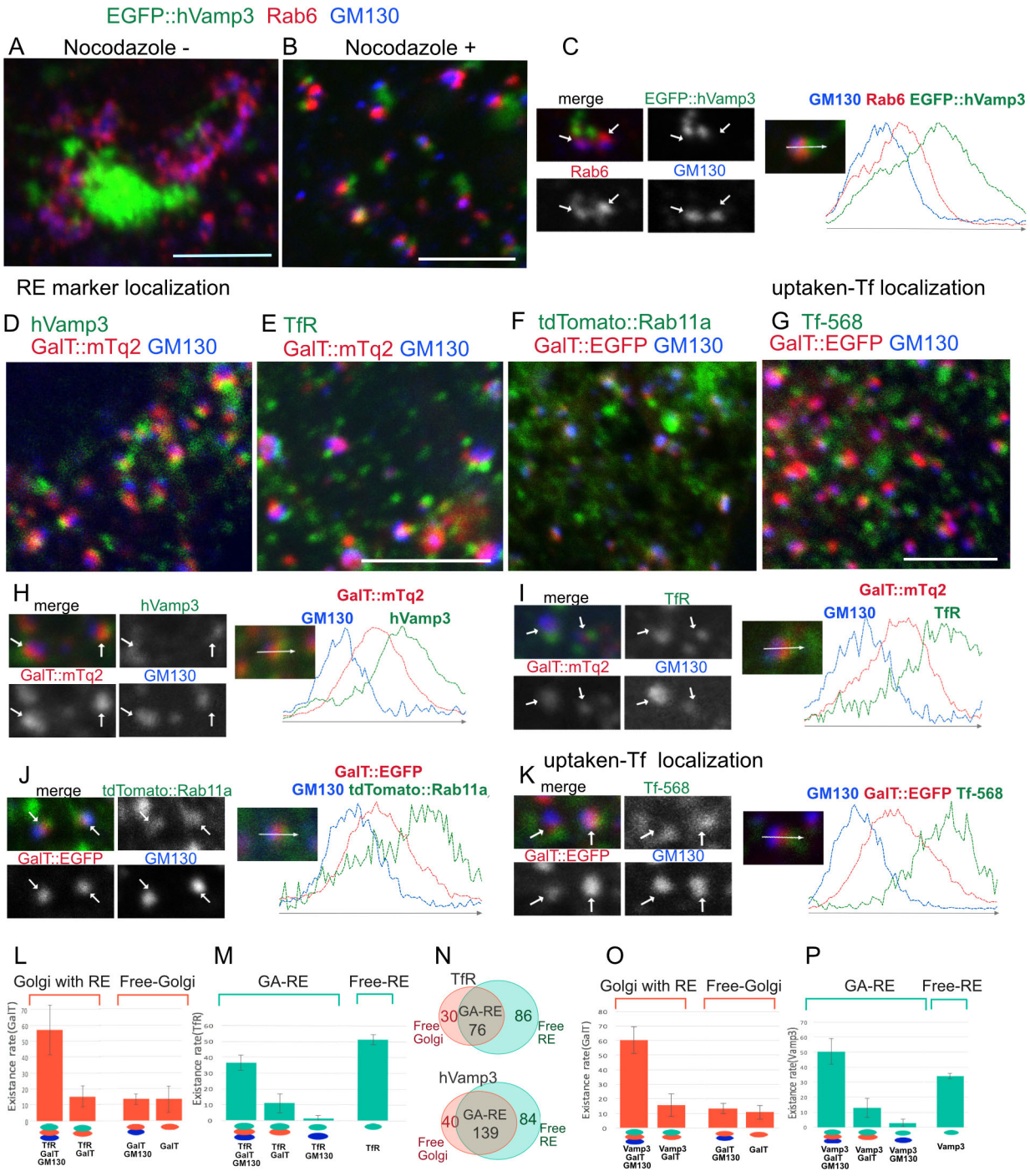

Fig. 4. REs attach to trans-side of Golgi stacks in HeLa cells. (A,B) HeLa cells expressing EGFP::hVamp3 (green) were incubated for 4 h without (A) or with (B) nocodazole, followed by immunostaining with anti-Rab6 (red), anti-GM130 (blue) antibodies. (C) Left panels indicate the examples of triple staining of Golgi stacks/REs (arrows). Plots show signal intensities from image on the left. Signal intensity was measured along the arrow (representing 1.5 µm) in inset, graph shows the overlap between channels. (D,E) HeLa cells expressing GalT::mTq2 (red) were treated for 4 h with nocodazole, followed by immunostaining with anti-GM130 (blue) and anti-Vamp3 (green) or TfR (green) antibodies. (F) HeLa cells expressing tdTomato::Rab11a (green) and GalT::EGFP (red) were incubated 4 h with nocodazole, followed by immunostaining with anti-GM130 antibody (blue). (G) HeLa cells expressing GalT::EGFP (red) were treated 4 h with nocodazole, pulse-labeled with Tf-568 (green) (10 min uptake and 20 min chase) and immunostained by anti-GM130 antibody (blue). (H–K) Left panels indicate the examples of triple-stained Golgi stacks/REs (arrows). Plots show signal intensities from image on the left. Signal intensity was measured along the arrow (representing 1.5 µm) in inset, graph shows the overlap between channels. (L,M) Percentages of GalT::mTq2-defined Golgi stacks (L) or TfR-defined REs (M) categorized by the association with other markers. (N) Venn diagrams of the numbers of GA-RE, free-Golgi and free-RE. RE is visualized by TfR (top) and Vamp3 (bottom). (O,P) Percentages of GalT::mTq2-defined Golgi stacks (O) or Vamp3-defined REs (P) categorized by the association with other markers. Scale bars: 5 µm.

RELCH–OSBP complex links REs with the TGN in mammalian cells treated with 25-hydrocholesterol – that mimics a cholesterol-starved state – and transfers cholesterol from REs to the TGN (Sobajima et al., 2018). However, the authors also showed that this association is limited to cells not treated with 25-hydrocholesterol (Sobajima et al., 2018). Without nocodazole treatment, REs in HeLa

Journal of Cell Science (2020) 133, jcs236935. doi:10.1242/jcs.236935

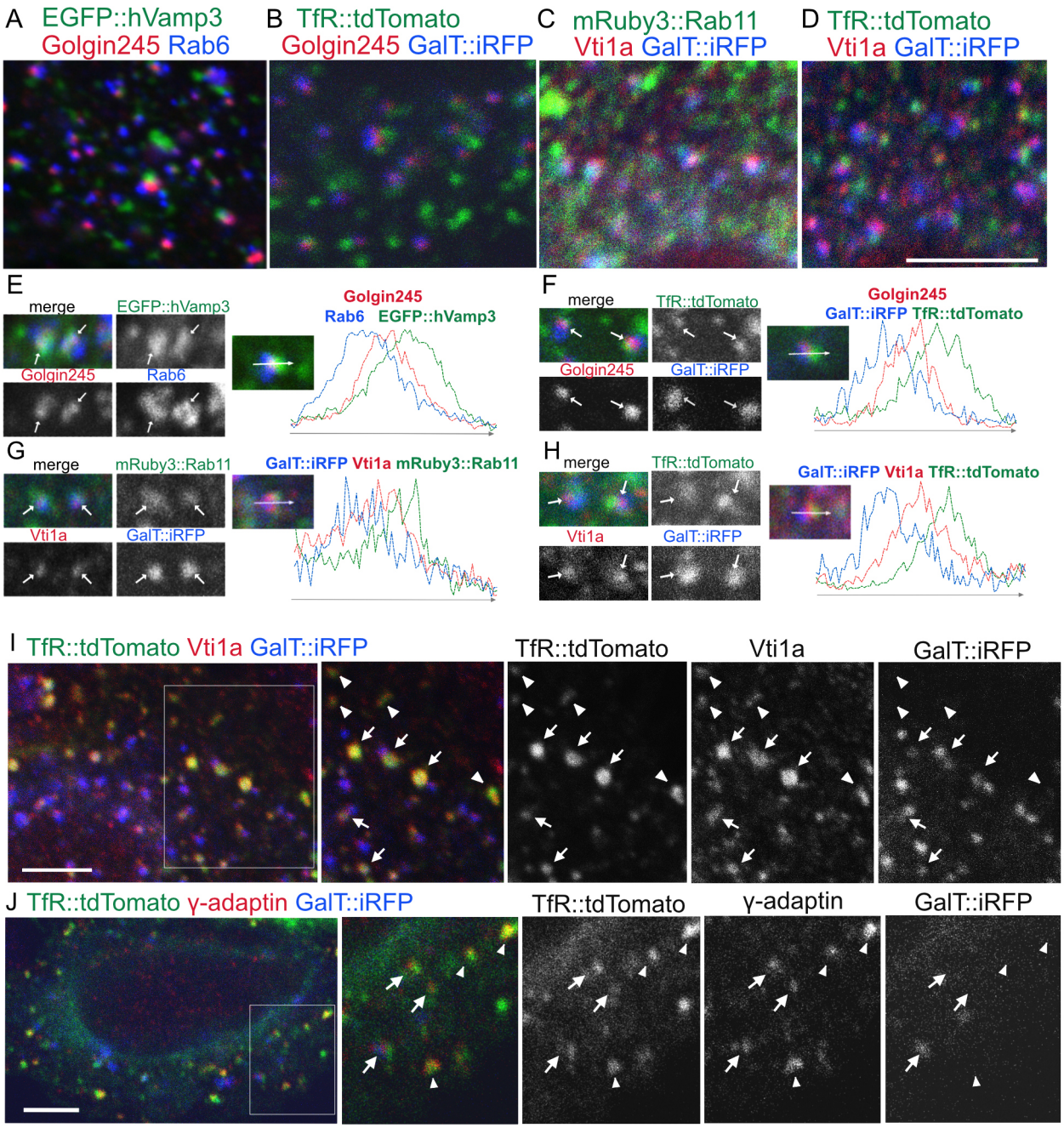

Fig. 5. Localization of REs and TGN markers in HeLa cells. (A) HeLa cells expressing EGFP::hVamp3 (green) were incubated 4 h with nocodazole and immunostained by anti-Golgin245 (red) and anti-Rab6 antibody (blue). (B) HeLa cells expressing TfR::tdTomato (green) and GalT::iRFP (blue) were incubated 4 h with nocodazole and immunostained by anti-Golgin245 antibody (red). (C,D) HeLa cells expressing mRuby3::Rab11 (C) or TfR::tdTomato (green) (D) and GalT::iRFP (blue) were incubated 4 h with nocodazole and immunostained by anti-Vti1a antibody (red). (E–H) Left panels are examples of triple-stained Golgi stacks or REs (arrows) by indicated antibodies or fluorescent proteins. Plots show signal intensities from image on the left. Signal intensity was measured along the arrow (representing 1.5 µm) in inset, graph shows the overlap between channels. (I,J) HeLa cells expressing TfR::tdTomato (green) and GalT::iRFP (blue) were incubated 4 h with nocodazole and immunostained by anti-Vti1a (I) or anti-γ adaptin antibody (red) (J). Boxed region within first panels are shown in magnification (1.22× in I and 1.89× in J) in the subsequent panels. Arrow indicate GA-REs. Arrowheads indicate free REs. Scale bars: 5 µm.

cells changed their shape and moved around too fast, and we were unable to examine the interaction between RE and Golgi even by SCLIM. Thus, we cannot exclude the possibility that Golgi-ribbons interact differently with REs in HeLa cells not treated with nocodazole. It is also important to investigate whether RELCH is responsible for RE associations with Golgi stacks in HeLa cells not treated with nocodazole, although there is no RELCH ortholog in the fly genome.

Existence of two RE states – Golgi-associated RE and free-RE

Our results collectively indicated that, in both *Drosophila* and MT-disrupted mammalian cells, REs occur in two distinct states, Golgi-associated RE and free-RE. These two states of REs are interconvertible: GA-REs often detach from Golgi stacks, whereas free-REs attach to Golgi stacks. In plants, it has already been established that there are two types of TGN – the GA-TGN and the free-TGN (Kang et al., 2011; Uemura and Nakano, 2013; Uemura et al., 2014; Viotti

Journal of Cell Science (2020) 133, jcs236935. doi:10.1242/jcs.236935

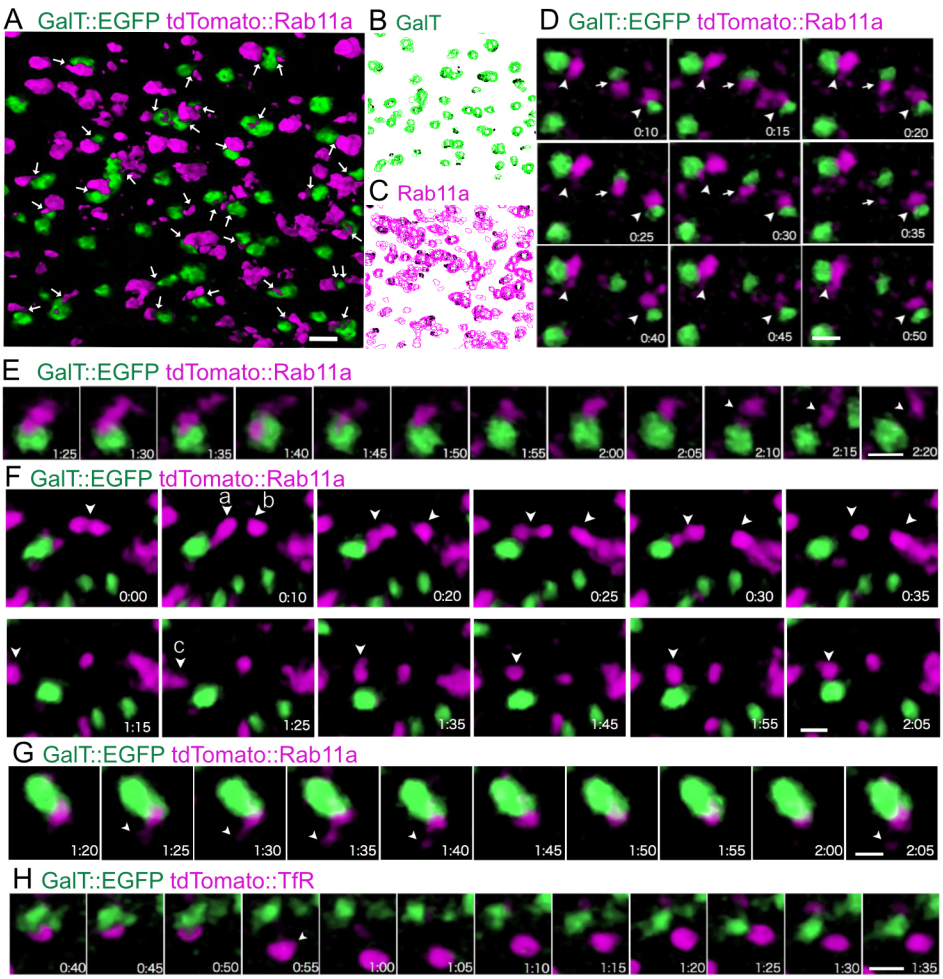

Fig. 6. Attachment and detachment of REs on the trans-side of Golgi stacks revealed by SCLIM. Frames of volume-rendered two-color 4D movies of HeLa cells expressing GalT::EGFP (trans-Golgi-cisternae: green) and tdTomato::Rab11a (RE: magenta) (A,D–G) or TfR::tdTomato (RE: magenta) (H) after 4 h of nocodazole treatment. (A) Frame obtained from Movie 2, showing free-REs, GA-REs and trans-Golgi-cisternae. Arrows indicate associations between Golgi and RE. (B,C) Motility of trans-Golgi-cisternae (B) and REs (C) obtained from Movie 2; shown is the outline of the objects in the first frame (black) and other frames (green or magenta). (D) Continuous associations (arrowheads) and spontaneous separation (arrows) of tdTomato::Rab11a (magenta) with GalT::EGFP (green). (E) Detachment of GA-RE. Part of an RE separating at 1:45, with the rest detaching at 2:20. Arrowheads indicate the detachment of RE from Golgi. (F) Division and fusion of free REs. At 0:00, a free RE (indicated by an arrowhead) divided into two. At 0:10, the left part (a) fused to small GA-RE, followed by detachment of the entire GA-RE from Golgi (0:35). Simultaneously, the right part of the RE (b) divided at 0:10 and fused with a larger RE on the right (at 0:25). At 1:25 another RE (c) appeared from the left and attached to the trans-Golgi cisternae (1:55). (G) Small vesicles budding from GA-RE visualized by tdTomato::Rab11a. (H) The entire RE detachment (0:55, arrowhead) and reattachment (1:25) to trans-Golgi. All times are shown as min:s in D–H. Scale bars: 1 µm (A,D–H).

et al., 2010). GA-TGNs occasionally peel off from Golgi stacks to become free-TGNs. By contrast, free-TGNs can attach to the Golgi stacks to become GA-TGNs. Although REs are not well defined in plants, Naramoto et al. (2014) discussed that the TGN or its subdomain might be the organelle that is functionally homologous to mammalian RE. In particular, the plant TGN receives endocytosed material and recycles it to the cell surface (Dettmer et al., 2006; Uemura, 2016). Furthermore, one of the plant Rab11 homologs (Ara4A) localizes to the TGN (Kang et al., 2011), although there are many Rab11 homologs in plants. In our study, we observed the dynamics of RE and Golgi stacks in both *Drosophila* and mammalian cells, and found a strong similarity to those of TGN and Golgi stacks reported in plants. Thus, fly and mammalian REs might be the functional counterpart of the TGN in plants. Both animal REs and plant TGNs are likely to be heterogeneous populations with different levels of maturation. Golgi-associated and Golgi-independent states of RE and TGN might be related to the progression of sorting events (Hernández-González et al., 2018; Uemura et al., 2019). The terminology ‘RE’ and ‘TGN’ might be further considered on the basis of homogeneity and difference between various species considering the molecular, functional, morphological and dynamical aspects.

Yeasts have separated Golgi cisternae, which have been shown to mature gradually (Casler et al., 2019; Kurokawa et al., 2019; Losev et al., 2006; Matsuura-Tokita et al., 2006). A recent study using yeast described the precise dynamics of Golgi and TGN transitions, and showed the presence of three successive stages – the glycosylating ‘Golgi stage’, the retrograde-cargo receiving ‘early TGN stage’ and the anterograde-cargo exporting ‘late TGN stage’ (Tojima et al., 2019). Consistent with this idea, we found that, in *Drosophila* and HeLa cells, Golgin245 and Vti1a, the tethering factor and the SNARE mediating retrograde traffic on the TGN, were distributed slightly closer to the cis-Golgi than the transport carrier component γ adaptin, which largely colocalizes with RE markers in GA-REs. This similarity between the yeast late-TGN and animal GA-RE may reflect the common mechanisms that underlie Golgi transport in eukaryote cells.

EGFP::GPI but not VSV-G::EGFP is transported through Golgi-attached RE

The substantial localization of GPI to GA-REs indicates that GPI travels through GA-REs and free-REs before reaching the plasma membrane. By contrast, VSV-G did not colocalize with RE and, presumably, is transported directly to the plasma membrane. These results suggest that GPI and VSV-G are sorted at the boundary between the trans-side of the Golgi stack and GA-REs. It is important to investigate where GPI and VSV-G start to segregate within the Golgi stack and GA-RE. It has been reported that TfR and Lamp1 segregate during the early stage of Golgi transport (Chen et al., 2017), and similar segregation might occur between GPI and VSV-G. Future studies, using two-color RUSH for GPI and VSV-G might, therefore, reveal their sorting mechanisms.

MATERIALS AND METHODS

Construction of plasmids

The puromycin-resistant gene in pMT-puro (Addgene plasmid #17923, deposited by David Sabatini) was replaced with a hygromycin-B-resistant gene in EGFP-DRD4 (Addgene plasmid #24100, deposited by Jean-Michel Arrang; Jeanneteau et al., 2004) to create pMT-hyg. The mTurquoise2::GalT

Journal of Cell Science (2020) 133, jcs236935. doi:10.1242/jcs.236935

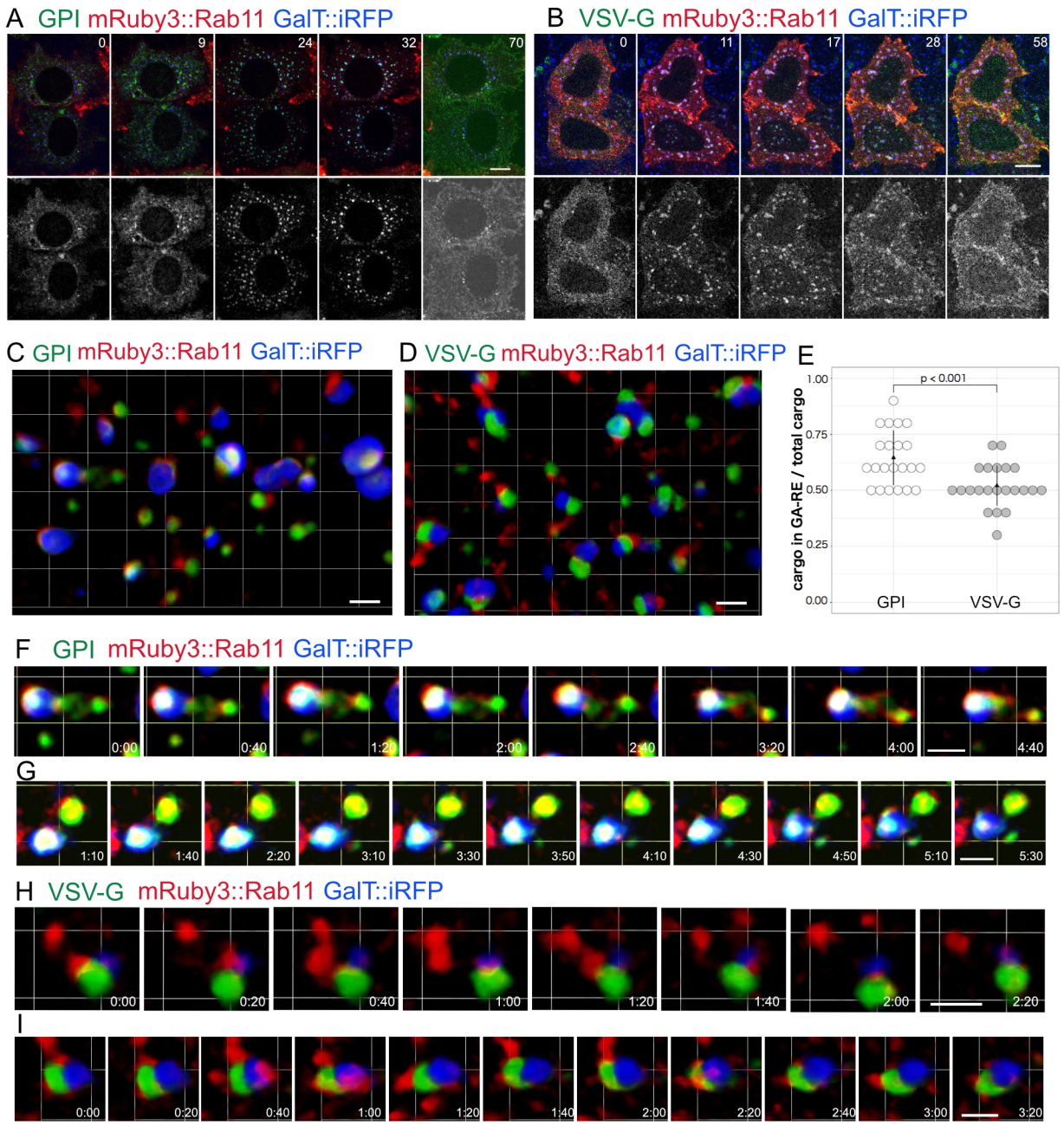

Fig. 7. GPI but not VSV-G localizes in Golgi-attached RE. Frames of volume-rendered two-color 4D movies of HeLa cells expressing ss::SBP::EGFP::GPI (GPI) (A,C,F,G) or VSV-G::SBP::EGFP (VSV-G) (B,D,H,I) (green), ss::streptavidin::KDEL or Ii::streptavidin (not visualized), GalT::iRFP (trans-Golgi-cisternae: blue) and mRuby3::Rab11a (RE: red) after 4 h nocodazole treatment. (A,B) Time of the transport of GPI (A) or VSV-G (B). The number on the right-upper corner of each image indicates the time point (min) after addition of biotin. Lower pictures show only cargo localizations. (C,D) Frames from Movie 5 that represent the localization of GPI at 25 min (C) or VSV-G at 28 min (D) close to Golgi stacks after addition of biotin. (E) The plot shows the association of GA-RE with cargo proteins GPI (white circles) or VSV-G (gray circles). Each circle represents one Golgi stack. (F) Frames from Movie 6 showing intense interaction of GA-RE and free-RE with GPI. (G) Frames of volume-rendered two-color 4D movies of HeLa cells expressing GPI at 60 min after biotin-addition. Not only the RE tubule but also the GPI-positive tubule is visible. (H) Frames from Movie 6 showing intense interaction of GA-RE and free-RE without VSV-G. (I) Frames of volume-rendered two-color 4D movies of HeLa cells expressing VSVG at 28 min after addition of biotin. Time is shown as min:s in F–I. Scale bars: 1 µm.

fragment in pmTurquoise2-Golgi (Addgene plasmid #36205, deposited by Dorus Gadella; Goedhart et al., 2012) was cloned into pMT-puro to build pMT-GalT-mTq2. By replacing mTq2 in pMT-GalT-mTq2 with EGFP and tdTomato in tdTomato-Rab11a-7 (Addgene plasmid #58128, deposited by Michael Davidson), pMT-GalT-EGFP and pMT-GalT-tdTomato were built.

From pEGFP-VAMP3 (Addgene plasmid #42310, deposited by Galli et al., 1998), DNA fragment encoding EGFP::hVamp3 was amplified and cloned into pMT-puro to create pMT-EGFP-hVamp3. *Drosophila* genomic DNA containing entire coding region of the synaptobrevin (*Syb*) gene were amplified and replaced hVamp3 within pMT-EGFP-hVamp3 to build pMT-EGFP-Syb. *Drosophila* Rab11 and mTurquoise2 were cloned into pMT-puro to build pMT-mTq2-Rab11. To build pMT-HA-Rab11, N-terminal 3×HA-tag (MYPYDVPDYAGGYPYDVPDYAGGYPYDVPDYAGGGGSGGG) followed by *Drosophila* Rab11 cDNA was cloned into pMT-puro. The myc::APEX2::myc fragment from pMT-myc-APEX2-myc (Otsuka et al., 2019) was inserted to pMT-hyg to create pMT-hyg-myc-APEX2-myc. The second Myc-tag in pMT-hyg-myc-APEX2-myc was replaced by EGFP to generate pMT-hyg-myc-APEX2-EGFP, then the first Myc-tag was replaced

by aa 1–59 of the human *B4GALT1* gene in pmTurquoise2-Golgi to create pMT-hyg-GalT-APEX2-EGFP. To build pMT-GalT-EGFP-T2A-tdTomato-Rab11, GalT::GFP from pMT-GalT-EGFP, the synthesized T2A sequence (ggaggtggaGAAGGACGCGGCAGCCTACTGACTTGCGGAGATGTCG-AAGAGAACCCTGGCCCTggtGccacc) and tdTomato::Rab11 form pUAST-tdTomato-Rab11-WT (Addgene plasmid #53473, deposited by Matthew Scott) were cloned into pMT-puro using Gibson-assembly.

To create p-element vectors pP{UAST-FLAG::hVamp3} and pP{UAST-FLAG::Syb} with the N-terminal 3×FLAG-tag (MDYKDHDGDYKDH-DIDYKDDDDKGGGSGG), hVamp3 and *Syb* gene fragments from pMT-EGFP-hVamp3 and pMT-EGFP-Syb were cloned into pUAST (Drosophila Genomics Resource Center, Bloomington, IN), respectively.

For expression in HeLa cells, CMV-GalT-EGFP and CMV-GalT-tdTomato were built by replacing mTq2 in pmTurquoise2-Golgi with EGFP and tdTomato. To create CMV-TfR-tdTomato, tagBFP2 in mTagBFP2-TFR-20 (Addgene plasmid #55327, deposited by Michael Davidson; Subach et al., 2011) was replaced by tdTomato. To generate stably transformed HeLa cells, episomal vectors based on pEBMulti-Puro TARGET tag-C (Wako) was used. For double transformants, the puromycin-resistant gene was replaced with a hygromycin-B-resistant gene in EGFP-DRD4 or neomycin-resistant gene in pEGFP-N1 to create pEB-hygro and pEB-neo, respectively. pEB-puro-GalT-EGFP was built by inserting GalT::EGFP fragment from pMT-GalT-EGFP into pEBMulti-Puro TARGET tag-C. pEB-hyg-tdTomato-Rab11a was built by cloning the DNA fragment coding tdTomato::Rab11a in tdTomato-Rab11a-7 into pEB-hyg. To create pEB-hyg-TfR-tdTomato, TfR::tdTomato fragment from CMV-TfR-tdTomato was cloned into pEB-hyg. EGFP in pEB-puro-GalT-EGFP was replaced by iRFP713 gene in piRFP (Addgene plasmid #31857, deposited by Vladislav Verkhusha; Filonov et al., 2011) and then GalT-iRFP713 fragment was moved to pEB-neo to construct pEB-neo-GalT-iRFP713. To construct CMV-mRuby3-Rab11a and CMV-HA-Rab11a, tdTomato in CMV-tdTomato-Rab11a-7 was replaced with two copies of the mRuby3 fragment from pKanCMV-mClover3-mRuby3 (Addgene plasmid #74252, deposited by Michael Lin; Bajar et al., 2016) or a HA-tag.

Immunostaining of S2 cells

Drosophila S2 cells were transiently transfected with pMT-mTq2-Rab11 using FuGENE HD (Promega). Expression was induced by adding 1 mM $CuSO_4$ at 2 days after transfection. Cells were fixed in 4% paraformaldehyde in 1×PBS for 1 h on ice and immunostaining of S2 cells was performed as described previously (Otsuka et al., 2019). Primary antisera were as follows: rabbit anti-GM130 (1:300; Abcam #ab30637, Cambridge, UK) and guinea pig anti-Rab6 (1:300) (Iwanami et al., 2016). Secondary antibodies were anti-rabbit and anti-guinea pig antibodies labeled with Alexa Fluor-568 and -647 (1:300) (Life Technologies, Carlsbad, CA). Imaging and data processing were the same as for fly retina immunostaining.

For images shown in Fig. 3A,B, S2 cells were transfected with pMK-V5-pcs (Otsuka et al., 2019) using FuGENE HD (Promega) and selected by using 100 µg/ml hygromycin B for 3 weeks to establish stable transformants. For double staining, cells were further transfected with pMT-HA-Rab11 and selected by using 2 µg/ml puromycin for 2 weeks. After induction by adding 1 mM $CuSO_4$ for 1 day, cells were fixed and immunostained with anti-V5, anti-Rab6, anti-GM130, anti-HA and anti-p120 antibodies.

Transgenic flies for UAS-FLAG::hVamp3 and UAS-FLAG::Syb

To generate transgenic flies, p-element vectors pP{UAST-FLAG::hVamp3} and pP{UAST-FLAG::Syb}were injected into *Drosophila* embryos using BestGene Inc. (Chino Hills, CA). Flies were grown at 20–25°C on standard cornmeal–glucose–agar–yeast food. To induce expression of FLAG::hVamp3, FLAG::Syb and GalT::ECFP in salivary glands or imaginal disks, transgenic flies with UAST-FLAG::hVamp3, UAST-FLAG::Syb or UAST- GalT::ECFP (Satoh et al., 2005) were crossed with hsp70-Gal4 flies, and F1 progenies were heat-shocked twice at 37°C for 20 min. For expression in retinas at early pupal stage, GMR-Gal4 or Elav-Gal4 were used.

Immunostaining of fly retinas, salivary glands and imaginal disks

Fixation and staining were performed as described previously with some modification (Satoh and Ready, 2005). Late pupal retinas at 80–100% pupal development (%pd), early pupal retinas at 20–30%pd (Satoh et al, 2005), salivary glands and imaginal disks were dissected in saline solution (2 mM KCl, 128 mM NaCl, 4 mM $MgCl_2$, 1.8 mM $CaCl_2$, 36 mM sucrose, 5 mM HEPES pH 7.1) using No.5 forceps, scissors (FST No.15010-11) and tungsten needles. Dissected tissues were fixed by incubation in fixative for 10–20 min at room temperature (RT). PLP (10 mM periodate, 75 mM lysine, 30 mM phosphate buffer, 4% paraformaldehyde) was used as fixative. After fixation, tissues were washed six to ten times with 1×PBS containing 0.3% Triton X-100 (PBST), followed by overnight incubation in primary antibody mixture (adequate concentration of antibodies, 5% bovine serum, 0.02% sodium azide in PBST) at 4°C. Next day, tissues were washed six to ten times with PBST, followed by incubation for 3–6 h in secondary antibody mixture (fluorescent dye-conjugated anti-mouse, rabbit, rat, guinea pig or goat antibodies, 5% bovine serum, 0.02% sodium azide in PBST) at RT. In the case of F-actin staining, Alexa Fluor-488 or -568 conjugated phalloidin was added to the primary antibody mixture. After incubation in secondary antibody mixture, tissues were washed six to ten times with PBST and mounted in 50% glycerol/1×PBS containing 0.25% n-propyl gallate.

Primary antisera were as follows: rabbit anti-GM130 (1:300; Abcam #ab30637), rabbit anti-MPPE (1:1000; gift from Dr Han, Southeast University, Nanjing, China), rat monoclonal anti-p120 (1:12; gift from Dr Goto, Rikkyo University) (Yamamoto-Hino et al., 2012), guinea pig anti-Rab6 (1:300; Iwanami et al., 2016), rat anti-Rab11 (1:250; Otsuka et al., 2019), goat anti-Golgin245 (1:500; Developmental Studies Hybridoma Bank), rabbit anti-AP1γ (1:2000; Hirst et al., 2009) and mouse monoclonal anti-FLAG (M2) (1:1000; Sigma-Aldrich-Japan, Tokyo, Japan). Secondary antibodies were anti-mouse, anti-rabbit, anti-rat, anti-goat and/or anti-guinea pig antibodies labeled with Alexa Fluor-488, -568 or -647 (1:300; Life Technologies). Images of samples were recorded using an FV1000 confocal microscope (PlanApo N 60×1.42 NA objective lens; Olympus, Tokyo, Japan). To minimize bleed-through, each signal in double- or triple-stained samples was imaged sequentially. Images were processed in accordance with the Guidelines for Proper Digital Image Handling using Fiji, Affinity Photo, and/or Adobe Photoshop CS3 (Adobe, San Jose, CA). To plot the immunostaining intensity across the Golgi stacks, the lines were drawn through each Golgi unit; plots with typical patterns are presented.

Electron microscopy imaging of myc::APEX2::Pcs and GalT::APEX2::EGFP

Drosophila S2 cells stably transformed by pMT-myc-APEX2-Pcs were transfected with pMT-hyg-GalT-APEX2-EGFP using FuGENE HD (Promega) and selected by 200 µg/ml hygromycin B for 3 weeks to establish myc-APEX2-Pcs/GalT-APEX2-EGFP double transformants. Expression of transgenes was induced by adding 0.5 mM $CuSO_4$ for 1 day.

Expression of myc::APEX2::Pcs and GalT::APEX2::EGFP was induced by adding 0.5 mM $CuSO_4$. Cells were fixed 16–18 h after induction. EM imaging of APEX2 was performed as described previously (Otsuka et al., 2019). Sections of 70–90 nm were imaged by using a JEM1400 transmission electron microscope (JEOL, Tokyo, Japan) operated at 80 kV, montage images were taken with a CCD camera system (JEOL).

Live imaging of S2 cells

S2 cells were transfected with pMT-GalT-EGFP-T2A-tdTomato-Rab11 and selected with puromycin as described above. Expression was induced by adding 0.5 mM $CuSO_4$ for 1 day. Cells were attached on the µ-Slide 8-well-chambered coverslip (ibidi, Martinsried, Germany) treated with poly-L-lysine (Merck, Darmstadt, Germany) and observed on an FV3000 confocal microscope equipped with a UPLSAPO60XS2 silicone-immersion 60× objective lens. Most of these cells showed the fluorescent signal of tdTomato::Rab11 in diffused pattern but some of them showed foci. Therefore, we performed live cell imaging of cells showing clear Rab11 foci. For each series, *z*-stacks (1 µm apart, three slices) were taken every 20 s for 20 min.

Immunostaining of HeLa cells

HeLa cells expressing fluorescent proteins were fixed in 4% paraformaldehyde in 1×PBS for 1 h on ice. Cells were rinsed three times for 2 min each in 1×PBS and then treated for 5 min in 1×PBS containing 0.1% Triton-X 100, followed by three 2-min rinses in 1×PBS. Cells were incubated for 2 h in primary

antibodies with 5% bovine serum in 1×PBS. After three rinses for 2 min each in 1×PBS, cells were incubated for 2 h in fluorescent dye-conjugated secondary antibodies with 5% bovine serum in 1×PBS. Imaging and data processing were performed as described for fly retina immunostaining. Primary antisera were as follows: Rabbit anti-GM130 (1:300; Abcam #ab30637, Cambridge, England), Rabbit anti-Rab6 (1:150; Abcam #ab95954), mouse anti-Golgin245 (1:250; #611280, BD Transduction Laboratories), mouse anti-γ adaptin (1:300; #610385BD, BD Transduction Laboratories), rabbit anti-Vamp3 (1:300) (#PA1-767A, Thermo Scientific, Waltham, MA) and mouse anti-human TfR (1:1000; #136800, Life Technologies). Secondary antibodies were anti-mouse and anti-rabbit antibodies labeled with Alexa Fluor-488, -568 or -647 (1:150; Life Technologies).

For quantification of the association between Golgi stacks and REs, HeLa cells were transiently transfected with pEGFP-VAMP3 or CMV-TfR-tdTomato using FuGENE HD. At 30–34 h after transfection, 10 µM of nocodazole was added to disrupt DNA; cells were fixed 4 h later. Under these experimental conditions, both Golgi stacks and fragmented REs were dispersed through the cytoplasm (Fig. 3B). Slides were immunostained using anti-Rab6 and anti-Golgin as described above. 2D confocal micrographs of immunostained cells were obtained by using an FV1000 confocal microscope. Each channel was binarized, then RE and Golgi cisternae were defined based on the area for the ellipse to fit, using ImageJ. When the ellipse objects with different markers overlapped, they were counted as associated.

Transferrin uptake in HeLa cells

After treatment with nocodazole for 4 h, GalT::EGFP-expressing HeLa cells were incubated with Alexa Fluor-568 conjugated to Tf (Tf-568; Life Technologies) for 20 min and then chased for 10 min in nocodazole-containing medium. Cells were then fixed and immunostained using anti-GM130 or anti-Golgin245 antibody and investigated whether endocytosed Tf localized to trans-side of Golgi stacks.

Stably transformed HeLa cells expressing fluorescent proteins

HeLa cells were transfected with pEB-GalT-EGFP using FuGENE HD. Cells were selected 48 h later by using 2 µg/ml puromycin (Wako) to establish stable transformants. These cells were transfected with pEB-hyg-tdTomato-Rab11a or pEB-hyg-TfR-tdTomato, and selected with 2 µg/ml of puromycin and 200 µg/ml of hygromycin B Gold (InvivoGen) to obtain double-transformants. Cells with strong expression were selected by limited dilution. For cells expressing GalT::iRFP, HeLa cells were transfected with pEB-neo-GalT-iRFP713 by using FuGENE HD (Promega), and selected using 500 ng/ml of G418 (Wako) to establish stable transformants. A clone with strong expression was selected using limited dilution.

Live imaging of HeLa cells using SCLIM

HeLa cells expressing the trans-Golgi marker (GalT::EGFP) and a RE marker (tdTomato::Rab11a or dTomato::TfR) were inoculated on glass-based dishes (Iwaki). Cells were cultured for 1 day in Phenol Red-free medium to reduce background fluorescence. Cells were then treated with 10 µM nocodazole for 4 h to disrupt microtubules, before observing them using super resolution confocal live imaging microscopy (SCLIM) (Kurokawa et al., 2013, 2019). *z*-stack images obtained through SCLIM were converted to 3D voxel data and processed by deconvolution with Volocity (Perkin Elmer) using the theoretical point-spread function for spinning-disk confocal microscopy. Volume-rendered images were generated using Volocity or FluoRender, and time-lapse series and movies were processed using ImageJ.

Synchronization of protein secretion by using the RUSH system

HeLa cells stably expressing GalT-iRFP were co-transfected with a DNA plasmid encoding mRuby3-Rab11 and the retention using selective hooks (RUSH) system bicistronic expression plasmids Str-Ii_VSVG-SBP-EGFP or Str-KDEL_SBP-EGFP-GPI (which were Addgene plasmids #65300 and 65294 deposited by Franck Perez; Boncompain et al., 2012) and jetPRIME were used according to the manufacturer's instructions (Polyplus transfection). After 6–10 h, 25 µM biliverdin was added. At 18–20 h after transfection, cells were treated with 2 µM brefeldin A and 10 µM nocodazole for 30 min to disrupt the Golgi apparatus and microtubules. Cells were washed five times in culture medium with 10 µM nocodazole and incubated for 2–5 h to regenerate mini-Golgi stacks. The streptavidin-binding peptide (SBP)–cargo proteins were released into the secretory pathway by replacing the medium with 50–100 µM biotin, 100 µg/ml cycloheximide and 10 µM nocodazole. 3D-stacks of confocal micrographs were obtained using SCLIM. 4D image volumes containing apparent GA-RE were selected. Each channel was binarized to define the regions containing mRuby3-Rab11 and SBP-EGFP–cargo by using ImageJ. The proportion of mRuby3 and EGFP double-positive areas in EGFP-positive areas was calculated.

Acknowledgements

We thank Dr Satoshi Goto (Rikkyo University, Tokyo, Japan) and Junhai Han (Southeast University, Nanjing, China) for kindly providing reagents. We also thank the Bloomington Drosophila Stock Center and the Drosophila Genomics and Genetic Resource (Kyoto Institute of Technology) for fly stocks. This work was made possible in part by using software funded by the NIH FluoRender (Visualization-Based and Interactive Analysis for Multichannel Microscopy Data, 1R01EB023947-01) and the National Institute of General Medical Sciences of the National Institutes of Health under grant number P41 GM103545-18.

Competing interests

The authors declare no competing or financial interests.

Author contributions

Conceptualization: T.S., A.K.S.; Methodology: S.F., K.K., T.S., A.K.S.; Formal analysis: S.F; Investigation: S.F., K.K., R.I., N.H., T.T., Y.N., T.S.; Data curation: S.F., T.S., A.K.S.; Writing - original draft: T.S., A.K.S.; Writing - review & editing: K.K., A.N.; Supervision: A.N., T.S., A.K.S.; Project administration: T.S., A.K.S.; Funding acquisition: K.K., A.N., T.S., A.K.S.

Funding

This work was supported by Precursory Research for Embryonic Science and Technology [grant no. 25-J-J4215], Japan Society for the Promotion of Science, KAKENHI [grant no. 15K07050], Sumitomo Foundation for Basic Science Research Projects, Astellas Foundation for Research on Metabolic Disorders and Female Researcher Joint Research Grant from Hiroshima University to A.K.S., KAKENHI [grant no. 19K06566] to T.S., and KAKENHI [grant nos 25221103, 17H06420 and 18H05275] to K.K. and A.N.

Supplementary information

Supplementary information available online at
http://jcs.biologists.org/lookup/doi/10.1242/jcs.236935.supplemental

References

Ang, A. L., Taguchi, T., Francis, S., Fölsch, H., Murrells, L. J., Pypaert, M., Warren, G. and Mellman, I. (2004). Recycling endosomes can serve as intermediates during transport from the Golgi to the plasma membrane of MDCK cells. *J. Cell Biol.* **167**, 531-543. doi:10.1083/jcb.200408165

Bajar, B. T., Wang, E. S., Lam, A. J., Kim, B. B., Jacobs, C. L., Howe, E. S., Davidson, M. W., Lin, M. Z. and Chu, J. (2016). Improving brightness and photostability of green and red fluorescent proteins for live cell imaging and FRET reporting. *Sci. Rep.* **6**, 20889. doi:10.1038/srep20889

Boncompain, G., Divoux, S., Gareil, N., de Forges, H., Lescure, A., Latreche, L., Mercanti, V., Jollivet, F., Raposo, G. and Perez, F. (2012). Synchronization of secretory protein traffic in populations of cells. *Nat. Methods* **9**, 493-498. doi:10.1038/nmeth.1928.10.1038/nmeth.1928

Burgess, J., Jauregui, M., Tan, J., Rollins, J., Lallet, S., Leventis, P. A., Boulianne, G. L., Chang, H. C., Le Borgne, R., Krämer, H. et al. (2011). AP-1 and clathrin are essential for secretory granule biogenesis in Drosophila. *Mol. Biol. Cell* **22**, 2094-2105. doi:10.1091/mbc.e11-01-0054

Casler, J. C., Papanikou, E., Barrero, J. J. and Glick, B. S. (2019). Maturation-driven transport and AP-1-dependent recycling of a secretory cargo in the Golgi. *J. Cell Biol.* **218**, 1582-1601. doi:10.1083/jcb.201807195

Chakrabarti, R., Joly, M. and Corvera, S. (1993). Redistribution of clathrin-coated vesicle adaptor complexes during adipocytic differentiation of 3T3-L1 cells. *J. Cell Biol.* **123**, 79-87. doi:10.1083/jcb.123.1.79

Chen, Y., Gershlick, D. C., Park, S. Y. and Bonifacino, J. S. (2017). Segregation in the Golgi complex precedes export of endolysosomal proteins in distinct transport carriers. *J. Cell Biol.* **216**, 4141-4151. doi:10.1083/jcb.201707172

Corthésy-Theulaz, I., Pauloin, A. and Pfeffer, S. R. (1992). Cytoplasmic dynein participates in the centrosomal localization of the Golgi complex. *J. Cell Biol.* **118**, 1333-1345. doi:10.1083/jcb.118.6.1333

Dettmer, J., Hong-Hermesdorf, A., Stierhof, Y.-D. and Schumacher, K. (2006). Vacuolar H+-ATPase activity is required for endocytic and secretory trafficking in Arabidopsis. *Plant Cell* **18**, 715-730. doi:10.1105/tpc.105.037978

Filonov, G. S., Piatkevich, K. D., Ting, L.-M., Zhang, J., Kim, K. and Verkhusha, V. V. (2011). Bright and stable near-infrared fluorescent protein for in vivo imaging. *Nat. Biotechnol.* **29**, 757-761. doi:10.1038/nbt.1918

Galli, T., Zahraoui, A., Vaidyanathan, V. V., Raposo, G., Tian, J. M., Karin, M., Niemann, H. and Louvard, D. (1998). A novel tetanus neurotoxin-insensitive vesicle-associated membrane protein in SNARE complexes of the apical plasma membrane of epithelial cells. *Mol. Biol. Cell* **9**, 1437-1448. doi:10.1091/mbc.9.6.1437

Gleeson, P. A., Anderson, T. J., Stow, J. L., Griffiths, G., Toh, B. H. and Matheson, F. (1996). p230 is associated with vesicles budding from the trans-Golgi network. *J. Cell Sci.* **109**, 2811-2821.

Goedhart, J., von Stetten, D., Noirclerc-Savoye, M., Lelimousin, M., Joosen, L., Hink, M. A., van Weeren, L., Gadella, T. W. J. and Royant, A. (2012). Structure-guided evolution of cyan fluorescent proteins towards a quantum yield of 93%. *Nat. Commun.* **3**, 751. doi:10.1038/ncomms1738

Goldenring, J. R. (2015). Recycling endosomes. *Curr. Opin. Cell Biol.* **35**, 117-122. doi:10.1016/j.ceb.2015.04.018

Gosavi, P. and Gleeson, P. A. (2017). The function of the Golgi ribbon structure - an enduring mystery unfolds! *Bioessays* **39**. doi:10.1002/bies.201700063

Granger, E., McNee, G., Allan, V. and Woodman, P. (2014). The role of the cytoskeleton and molecular motors in endosomal dynamics. *Semin. Cell Dev. Biol.* **31**, 20-29. doi:10.1016/j.semcdb.2014.04.011

Guo, Y., Zanetti, G. and Schekman, R. (2013). A novel GTP-binding protein-adaptor protein complex responsible for export of Vangl2 from the trans Golgi network. *eLife* **2**, e00160. doi:10.7554/eLife.00160

Hernández-González, M., Bravo-Plaza, I., Pinar, M., de Los Ríos, V., Arst, H. N., Jr and Peñalva, M. A. (2018). Endocytic recycling via the TGN underlies the polarized hyphal mode of life. *PLoS Genet.* **14**, e1007291. doi:10.1371/journal.pgen.1007291

Hierro, A., Gershlick, D. C., Rojas, A. L. and Bonifacino, J. S. (2015). Formation of tubulovesicular carriers from endosomes and their fusion to the trans-Golgi Network. *Int. Rev. Cell Mol. Biol.* **318**, 159-202. doi:10.1016/bs.ircmb.2015.05.005

Hirst, J., Sahlender, D. A., Choma, M., Sinka, R., Harbour, M. E., Parkinson, M. and Robinson, M. S. (2009). Spatial and functional relationship of GGAs and AP-1 in Drosophila and HeLa cells. *Traffic* **10**, 1696-1710. doi:10.1111/j.1600-0854.2009.00983.x

Horgan, C. P., Hanscom, S. R., Jolly, R. S., Futter, C. E. and McCaffrey, M. W. (2010). Rab11-FIP3 links the Rab11 GTPase and cytoplasmic dynein to mediate transport to the endosomal-recycling compartment. *J. Cell Sci.* **123**, 181-191. doi:10.1242/jcs.052670

Iwanami, N., Nakamura, Y., Satoh, T., Liu, Z. and Satoh, A. K. (2016). Rab6 Is required for multiple apical transport pathways but not the basolateral transport pathway in Drosophila photoreceptors. *PLoS Genet.* **12**, e1005828. doi:10.1371/journal.pgen.1005828

Jeanneteau, F., Diaz, J., Sokoloff, P. and Griffon, N. (2004). Interactions of GIPC with dopamine D2, D3 but not D4 receptors define a novel mode of regulation of G protein-coupled receptors. *Mol. Biol. Cell* **15**, 696-705. doi:10.1091/mbc.e03-05-0293

Kang, B.-H., Nielsen, E., Preuss, M. L., Mastronarde, D. and Staehelin, L. A. (2011). Electron tomography of RabA4b- and PI-4Kβ1-labeled trans Golgi network compartments in Arabidopsis. *Traffic* **12**, 313-329. doi:10.1111/j.1600-0854.2010.01146.x

Klumperman, J. (2011). Architecture of the mammalian Golgi. *Cold Spring Harb. Perspect. Biol.* **3**, a005181. doi:10.1101/cshperspect.a005181

Kreykenbohm, V., Wenzel, D., Antonin, W., Atlachkine, V. and von Mollard, G. F. (2002). The SNAREs vti1a and vti1b have distinct localization and SNARE complex partners. *Eur. J. Cell Biol.* **81**, 273-280. doi:10.1078/0171-9335-00247

Kurokawa, K., Ishii, M., Suda, Y., Ichihara, A. and Nakano, A. (2013). Live cell visualization of Golgi membrane dynamics by super-resolution confocal live imaging microscopy. *Methods Cell Biol.* **118**, 235-242. doi:10.1016/B978-0-12-417164-0.00014-8

Kurokawa, K., Osakada, H., Kojidani, T., Waga, M., Suda, Y., Asakawa, H., Haraguchi, T. and Nakano, A. (2019). Visualization of secretory cargo transport within the Golgi apparatus. *J. Cell Biol.* **218**, 1602-1618. doi:10.1083/jcb.201807194

Lock, J. G. and Stow, J. L. (2005). Rab11 in recycling endosomes regulates the sorting and basolateral transport of E-cadherin. *Mol. Biol. Cell* **16**, 1744-1755. doi:10.1091/mbc.e04-10-0867

Losev, E., Reinke, C. A., Jellen, J., Strongin, D. E., Bevis, B. J. and Glick, B. S. (2006). Golgi maturation visualized in living yeast. *Nature* **441**, 1002-1006. doi:10.1038/nature04717

Makaraci, P. and Kim, K. (2018). trans-Golgi network-bound cargo traffic. *Eur. J. Cell Biol.* **97**, 137-149. doi:10.1016/j.ejcb.2018.01.003

Martell, J. D., Deerinck, T. J., Lam, S. S., Ellisman, M. H. and Ting, A. Y. (2017). Electron microscopy using the genetically encoded APEX2 tag in cultured mammalian cells. *Nat. Protoc.* **12**, 1792-1816. doi:10.1038/nprot.2017.065

Matsuura-Tokita, K., Takeuchi, M., Ichihara, A., Mikuriya, K. and Nakano, A. (2006). Live imaging of yeast Golgi cisternal maturation. *Nature* **441**, 1007-1010. doi:10.1038/nature04737

Mayor, S., Presley, J. F. and Maxfield, F. R. (1993). Sorting of membrane components from endosomes and subsequent recycling to the cell surface occurs by a bulk flow process. *J. Cell Biol.* **121**, 1257-1269. doi:10.1083/jcb.121.6.1257

Misaki, R., Morimatsu, M., Uemura, T., Waguri, S., Miyoshi, E., Taniguchi, N., Matsuda, M. and Taguchi, T. (2010). Palmitoylated Ras proteins traffic through recycling endosomes to the plasma membrane during exocytosis. *J. Cell Biol.* **191**, 23-29. doi:10.1083/jcb.200911143

Naramoto, S., Otegui, M. S., Kutsuna, N., de Rycke, R., Dainobu, T., Karampelias, M., Fujimoto, M., Feraru, E., Miki, D., Fukuda, H. et al. (2014). Insights into the localization and function of the membrane trafficking regulator GNOM ARF-GEF at the Golgi apparatus in Arabidopsis. *Plant Cell* **26**, 3062-3076. doi:10.1105/tpc.114.125880

Otsuka, Y., Satoh, T., Nakayama, N., Inaba, R., Yamashita, H. and Satoh, A. K. (2019). Parcas is the predominant Rab11-GEF for rhodopsin transport in Drosophila photoreceptors. *J. Cell Sci.* **132**, jcs231431. doi:10.1242/jcs.231431

Papanikou, E. and Glick, B. S. (2014). Golgi compartmentation and identity. *Curr. Opin. Cell Biol.* **29**, 74-81. doi:10.1016/j.ceb.2014.04.010

Riedel, F., Gillingham, A. K., Rosa-Ferreira, C., Galindo, A. and Munro, S. (2016). An antibody toolkit for the study of membrane traffic in Drosophila melanogaster. *Biol. Open* **5**, 987-992. doi:10.1242/bio.018937

Rosenbaum, E. E., Vasiljevic, E., Cleland, S. C., Flores, C. and Colley, N. J. (2014). The Gos28 SNARE protein mediates intra-Golgi transport of rhodopsin and is required for photoreceptor survival. *J. Biol. Chem.* **289**, 32392-32409. doi:10.1074/jbc.M114.585166

Sakai, T., Yamashina, S. and Ohnishi, S.-I. (1991). Microtubule-disrupting drugs blocked delivery of endocytosed transferrin to the cytocenter, but did not affect return of transferrin to plasma membrane. *J. Biochem.* **109**, 528-533. doi:10.1093/oxfordjournals.jbchem.a123415

Satoh, A. K. and Ready, D. F. (2005). Arrestin1 mediates light-dependent rhodopsin endocytosis and cell survival. *Curr. Biol.* **15**, 1722-1733. doi:10.1016/j.cub.2005.08.064

Satoh, A. K., O'Tousa, J. E., Ozaki, K. and Ready, D. F. (2005). Rab11 mediates post-Golgi trafficking of rhodopsin to the photosensitive apical membrane of Drosophila photoreceptors. *Development* **132**, 1487-1497. doi:10.1242/dev.01704

Schneider, I. (1972). Cell lines derived from late embryonic stages of Drosophila melanogaster. *J. Embryol. Exp. Morphol.* **27**, 353-365.

Sobajima, T., Yoshimura, S.-I., Maeda, T., Miyata, H., Miyoshi, E. and Harada, A. (2018). The Rab11-binding protein RELCH/KIAA1468 controls intracellular cholesterol distribution. *J. Cell Biol.* **217**, 1777-1796. doi:10.1083/jcb.201709123

Subach, O. M., Cranfill, P. J., Davidson, M. W. and Verkhusha, V. V. (2011). An enhanced monomeric blue fluorescent protein with the high chemical stability of the chromophore. *PLoS ONE* **6**, e28674. doi:10.1371/journal.pone.0028674

Tojima, T., Suda, Y., Ishii, M., Kurokawa, K. and Nakano, A. (2019). Spatiotemporal dissection of the trans-Golgi network in budding yeast. *J. Cell Sci.* **132**, jcs231159. doi:10.1242/jcs.231159

Uemura, T. (2016). Physiological roles of plant post-Golgi transport pathways in membrane trafficking. *Plant Cell Physiol.* **57**, 2013-2019. doi:10.1093/pcp/pcw149

Uemura, T. and Nakano, A. (2013). Plant TGNs: dynamics and physiological functions. *Histochem. Cell Biol.* **140**, 341-345. doi:10.1007/s00418-013-1116-7

Uemura, T., Suda, Y., Ueda, T. and Nakano, A. (2014). Dynamic behavior of the trans-golgi network in root tissues of Arabidopsis revealed by super-resolution live imaging. *Plant Cell Physiol.* **55**, 694-703. doi:10.1093/pcp/pcu010

Uemura, T., Nakano, R. T., Takagi, J., Wang, Y., Kramer, K., Finkemeier, I., Nakagami, H., Tsuda, K., Ueda, T., Schulze-Lefert, P. et al. (2019). A Golgi-released subpopulation of the trans-golgi network mediates protein secretion in Arabidopsis. *Plant Physiol.* **179**, 519-532. doi:10.1104/pp.18.01228

Ullrich, O., Reinsch, S., Urbé, S., Zerial, M. and Parton, R. G. (1996). Rab11 regulates recycling through the pericentriolar recycling endosome. *J. Cell Biol.* **135**, 913-924. doi:10.1083/jcb.135.4.913

van Ijzendoorn, S. C. D. (2006). Recycling endosomes. *J. Cell Sci.* **119**, 1679-1681. doi:10.1242/jcs.02948

Viotti, C., Bubeck, J., Stierhof, Y.-D., Krebs, M., Langhans, M., van den Berg, W., van Dongen, W., Richter, S., Geldner, N., Takano, J. et al. (2010). Endocytic and secretory traffic in Arabidopsis merge in the trans-Golgi network/early endosome, an independent and highly dynamic organelle. *Plant Cell* **22**, 1344-1357. doi:10.1105/tpc.109.072637

Wei, J.-H. and Seemann, J. (2017). Golgi ribbon disassembly during mitosis, differentiation and disease progression. *Curr. Opin. Cell Biol.* **47**, 43-51. doi:10.1016/j.ceb.2017.03.008

Yamamoto-Hino, M., Abe, M., Shibano, T., Setoguchi, Y., Awano, W., Ueda, R., Okano, H. and Goto, S. (2012). Cisterna-specific localization of glycosylation-related proteins to the Golgi apparatus. *Cell Struct. Funct.* **37**, 55-63. doi:10.1247/csf.11037

Yamashiro, D. J. and Maxfield, F. R. (1987). Acidification of morphologically distinct endosomes in mutant and wild-type Chinese hamster ovary cells. *J. Cell Biol.* **105**, 2723-2733. doi:10.1083/jcb.105.6.2723